Eastern North Pacific Hurricane Season of 2006

RICHARD J. PASCH, ERIC S. BLAKE, LIXION A. AVILA, JOHN L. BEVEN, DANIEL P. BROWN,
JAMES L. FRANKLIN, RICHARD D. KNABB, MICHELLE M. MAINELLI, JAMIE R. RHOME, AND
STACY R. STEWART

Tropical Prediction Center/National Hurricane Center, NOAA/NWS/NCEP, Miami, Florida

ABSTRACT

The hurricane season of 2006 in the eastern North Pacific basin is summarized, and the individual tropical cyclones are described. Also, the official track and intensity forecasts of these cyclones are verified and evaluated. The 2006 eastern North Pacific season was an active one, in which 18 tropical storms formed. Of these, 10 became hurricanes and 5 became major hurricanes. A total of 2 hurricanes and 1 tropical depression made landfall in Mexico, causing 13 direct deaths in that country along with significant property damage. On average, the official track forecasts in the eastern Pacific for 2006 were quite skillful. No appreciable improvement in mean intensity forecasts was noted, however.

1. Overview

After three consecutive below-average hurricane seasons, tropical cyclone activity in the eastern North Pacific basin was above average in 2006. A total of 18 tropical storms developed, and 10 of these strengthened into hurricanes (Table 1; Fig. 1). Five of the hurricanes intensified into major hurricanes [category 3 or stronger on the Saffir–Simpson hurricane scale (Saffir 1973; Simpson 1974)]. These totals are above the 1971–2005 means of 15 tropical storms, 9 hurricanes, and 4 major hurricanes. Not since the 1992 season have as many as 18 tropical storms been observed, and the last time 10 hurricanes occurred in an eastern North Pacific season was 1993. Moreover, the 2006 total of 5 major hurricanes equals the highest seen since 1998. Three tropical depressions that did not strengthen into tropical storms also formed during the season. After two years without hurricane strikes, the 2006 season featured several landfalls in Mexico. One major hurricane (Lane), one category 2 hurricane (John), and one tropical depression (Paul) made landfall in Mexico during the season.

One metric to gauge the overall activity of a season is the Accumulated Cyclone Energy (ACE) index. It is calculated by summing up the squares of the wind speeds in knots every 6 h for all tropical and subtropical cyclones while at or above tropical storm strength. The ACE for 2006 in the eastern North Pacific was 120×10^4 kt^2, or about 107% of the long-term (1971–2005) mean. Although the ACE value for 2006 was just slightly above average, it was the highest observed since 1998. One possible reason for the above-normal activity in 2006 is the development of an El Niño episode during the season (Levinson 2007).

The 2006 season started close to the average date, with a tropical storm (Aletta) developing in late May just a couple days ahead of the long-term (1971–2005) median start date of 29 May. However, a full six weeks passed until the formation of the second tropical storm during the second week of July. The formation of Bud ushered in an active period for tropical cyclones; 10 tropical storms formed during July and August, 3 more than normal during this period. After a slightly below-average September, five tropical storms formed during October–November 2006. This is well above the long-term (1971–2005) mean of about two. Two tropical storms formed during November, which tied the record for number of formations in that month, held by 1966.

As noted by Knabb et al. (2008), the clustered nature of some eastern North Pacific seasons can be attributed in part to the Madden–Julian oscillation (MJO; Madden and Julian 1972). Analysis of 200-mb velocity potential anomalies (Fig. 2) indicates that most tropical cyclone genesis points during 2006 coincided with the

Corresponding author address: Dr. Richard J. Pasch, National Hurricane Center, 11691 SW 17th St., Miami, FL 33165.
E-mail: richard.j.pasch@noaa.gov

TABLE 1. Eastern North Pacific tropical storms and hurricanes of 2006.

Name	Class*	Dates**	Max 1-min wind (kt)	Min SLP (mb)	Direct deaths
Aletta	T	27–30 May	40	1002	
Bud	H	11–16 Jul	110	953	
Carlotta	H	12–16 Jul	75	981	
Daniel	H	16–26 Jul	130	933	
Emilia	T	21–28 Jul	55	990	
Fabio	T	31 Jul–3 Aug	45	1000	
Gilma	T	1–3 Aug	35	1004	
Hector	H	15–23 Aug	95	966	
Ileana	H	21–27 Aug	105	955	
John	H	28 Aug–4 Sep	115	948	5
Kristy	H	30 Aug–8 Sep	70	985	
Lane	H	13–17 Sep	110	952	4
Miriam	T	16–18 Sep	40	999	
Norman	T	9–15 Oct	45	1000	
Olivia	T	9–12 Oct	40	1000	
Paul	H	21–26 Oct	90	970	4
Rosa	T	8–10 Nov	35	1002	
Sergio	H	13–20 Nov	95	965	

* Tropical storm (T), wind speed 34–63 kt (17–32 m s^{-1}); Hurricane (H), wind speed 64 kt (33 m s^{-1}) or higher.
** Dates are based on UTC and include the tropical depression stage, but exclude the remnant low stage.

upper-level divergent phases of the MJO over the eastern North Pacific. In addition, only one of the tropical cyclones that did form outside of the upper-level divergent phase became a hurricane (John, which formed on 28 August). Using satellite data analysis techniques described by Avila et al. (2003), the genesis of most of the tropical cyclones in the eastern North Pacific during 2006 can be attributed, at least in part, to westward-moving tropical waves that originated from Africa and crossed Central America. These tropical waves, with their focused source of low-level vorticity, propagated into the eastern North Pacific throughout the hurricane season as usual. However, they led to the development of more tropical cyclones during the upper-level divergent phases of the MJO, which provided an environment more conducive for convection. It should be noted, however, that this MJO signal is often not as well defined as it was in 2006, which makes it difficult for forecasters to use such diagrams in real time.

A summary of the life cycle of each of the 2006 season's tropical cyclones is provided in section 2. Section 3 provides verification statistics on official National Hurricane Center (NHC) forecasts.

2. Tropical cyclone summaries

Summaries of individual cyclones in this section are based on NHC's poststorm meteorological analyses.

These analyses result in the creation of a "best-track" database for each storm, consisting of 6-hourly representative estimates of the cyclone's center location, maximum sustained (1-min average) surface (10 m) wind, and minimum sea level pressure. The life cycle of each cyclone (corresponding to the dates given in Table 1 for the season's tropical storms and hurricanes) is defined to include the tropical depression stage, but it does not include the remnant low stage. The tracks for the season's tropical storms and hurricanes, including their tropical depression and remnant low stages (if applicable), are shown in Fig. 1.

Observations of eastern North Pacific tropical cyclones are generally limited to satellite data, primarily from the Geostationary Operational Environmental Satellites (GOES). GOES-East and GOES-West provide the visible and infrared imagery that serves as input for intensity estimates using the Dvorak (1984) classification technique. This imagery is supplemented by occasional microwave satellite data and imagery from the National Oceanic and Atmospheric Administration (NOAA) polar-orbiting satellites, the Defense Meteorological Satellite Program (DMSP) satellites, the National Aeronautics and Space Administration (NASA) Tropical Rainfall Measuring Mission (TRMM), and the NASA Quick Scatterometer (QuikSCAT), among others. While passive microwave imagery is useful for tracking tropical cyclones and assessing their structure, QuikSCAT retrieves estimates of ocean surface vector winds across a fairly wide swath, and with careful interpretation it can provide occasional estimates of the location, intensity, and outer wind radii of a tropical cyclone. The 53rd Weather Reconnaissance Squadron of the U.S. Air Force Reserve Command (AFRC) flew several reconnaissance missions into eastern North Pacific tropical cyclones during 2006: three in Hurricane John, two in Hurricane Lane, and two in Hurricane Paul. Land-based radars from the Meteorological Service of Mexico were also extremely useful for monitoring tropical cyclones during 2006.

a. Tropical Storm Aletta, 27–30 May

A tropical wave moved from Central America into the eastern North Pacific Ocean on 21 May, and moved very slowly westward for the next several days. On 23–24 May, the wave interacted with a large low-level cyclonic circulation near the Gulf of Tehuantepec, and deep convection increased. By 25 May, a broad surface low had formed a few hundred nautical miles to the south of Acapulco, Mexico. Vertical shear, due in part to strong upper-tropospheric southwesterly winds over the area, inhibited development of this nearly stationary low for a couple of days. By early on 27 May, how-

ever, the shear lessened slightly, and the system became organized into a tropical depression centered about 165 n mi southwest of Acapulco around 0600 UTC. By 1800 UTC that day, convective banding features became more prominent and the system strengthened into a tropical storm. Aletta's estimated peak intensity of 40 kt was reached by 0600 UTC 28 May, while the storm was centered about 110 n mi southwest of Acapulco.

Initially the cyclone moved northeastward toward the coast of Mexico, but a weak midlevel ridge soon impeded this motion. By early on 28 May, Aletta turned toward the west. Steering currents then became weak and ill-defined, and it is estimated that the center moved in a small counterclockwise loop for about a day. On 29 May, Aletta began to drift generally westward, while increased westerly shear and an incursion of dry, stable air caused the cyclone to weaken to a tropical depression by 1800 UTC. As the system moved slowly west-northwestward it continued to weaken, and it degenerated to a remnant low by 0000 UTC 31 May. This low dissipated soon thereafter.

b. Hurricane Bud, 11–16 July

Bud developed from a tropical wave that emerged from the west coast of Africa on 27 June and reached the eastern North Pacific basin by 7 July. An area of surface low pressure formed along the wave on 9 July approximately 550 n mi south of Manzanillo, Mexico. Showers and thunderstorms associated with the low gradually became better organized, and early on 11 July a tropical depression formed approximately 700 n mi south of Cabo San Lucas, Mexico.

The tropical cyclone moved west-northwestward throughout its entire life span, with steering provided by a persistent midlevel subtropical ridge extending westward from northern Mexico. Initially, early on 11 July, the depression encountered northerly wind shear. The shear decreased later that day, however, and the cyclone developed rapidly over warm waters, reaching hurricane strength very late that evening. Intensification continued on 12 July, as outer bands dissipated while inner-core convection consolidated and an eye became clearly evident (Fig. 3). Bud became a major hurricane on 13 July, reaching its estimated maximum intensity of 110 kt (category 3) that day about 650 n mi west-southwest of Cabo San Lucas. Thereafter, Bud encountered cooler waters and stable air that induced rapid weakening. Bud dropped below hurricane strength early on 14 July, and it lost much of its deep convection later that day. Bud weakened to a depression early on 15 July and degenerated into a remnant low pressure area the next day. The low dissipated

within the low-level easterly trade winds on 17 July about 650 n mi east-northeast of Hawaii.

c. Hurricane Carlotta, 12–16 July

Carlotta formed from a tropical wave that moved off the coast of Africa on 30 June. Convection associated with the wave, which had been minimal, increased as the system entered the eastern Pacific on 9 July. By late on 10 July, the wave had developed a closed area of surface low pressure. Showers and thunderstorms increased over a broad area to the south of Acapulco the following day, and by 0000 UTC 12 July, when the low was located about 250 n mi south of Zihuatanejo, Mexico, the deep convection had enough organization for the system to be designated a tropical depression.

Moving briskly west-northwestward to the south of midlevel high pressure over northwestern Mexico, the cyclone strengthened quickly under a deep burst of central convection early on 12 July and became a tropical storm at 0600 UTC about 230 n mi south-southwest of Zihuatanejo. It became a hurricane 24 h later, about 375 n mi south of Cabo San Lucas. Carlotta had a large circulation initially, and its outer rainbands scraped the Mexican coast from the Gulf of Tehuantepec to Manzanillo on 12 July.

As Carlotta strengthened in an environment of light vertical wind shear and warm waters, the system became more compact. On 13 July the forward motion began to slow while some northwesterly shear—in part from the outflow of Hurricane Bud located about 600 n mi to the west of Carlotta—slowed the intensification rate. Carlotta developed a banding eye and reached its peak intensity of 75 kt late on 13 July, but northwesterly mid- to upper-level shear increased and Carlotta weakened, becoming a tropical storm at 1800 UTC 14 July about 350 n mi southwest of Cabo San Lucas. With the northern portion of the circulation over cooler waters, convection began to decrease, and it appeared that Carlotta's decay stage had begun. However, wind shear may have decreased and there was a resurgence of convection overnight; an eye redeveloped and Carlotta is estimated to have regained hurricane strength near 0000 UTC 15 July.

Within a few hours of regaining hurricane strength, Carlotta, continuing west-northwestward, crossed the 26°C SST isotherm, and the eye disappeared. Carlotta weakened again to a tropical storm at 1200 UTC 15 July. Decay this time was swift and uninterrupted. Carlotta weakened to a tropical depression 24 h later, about 640 n mi west-southwest of Cabo San Lucas. Unable to generate deep convection over 23°C water, Carlotta degenerated to a remnant low by 0000 UTC 17 July. The remnant low moved slowly westward for an-
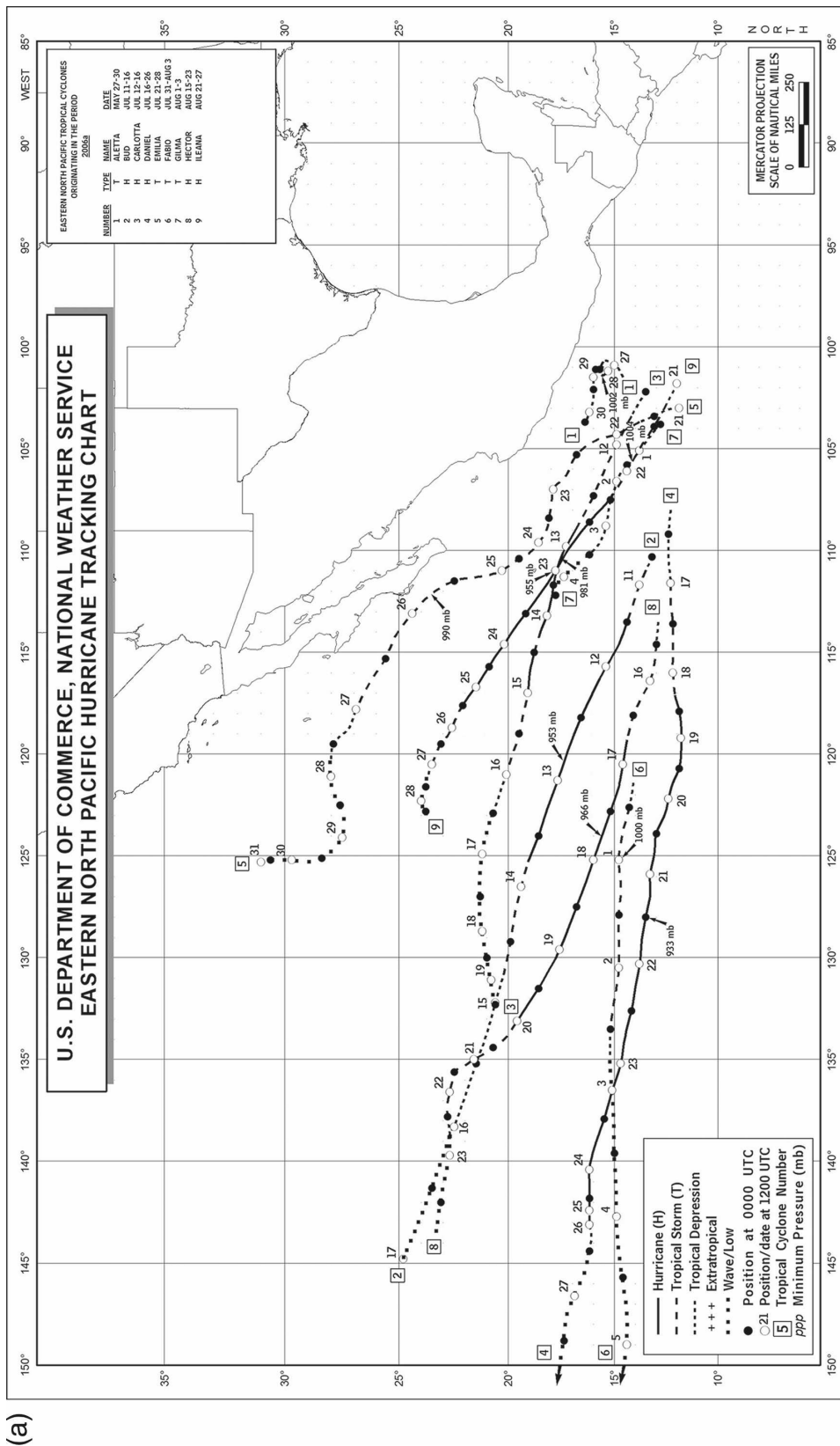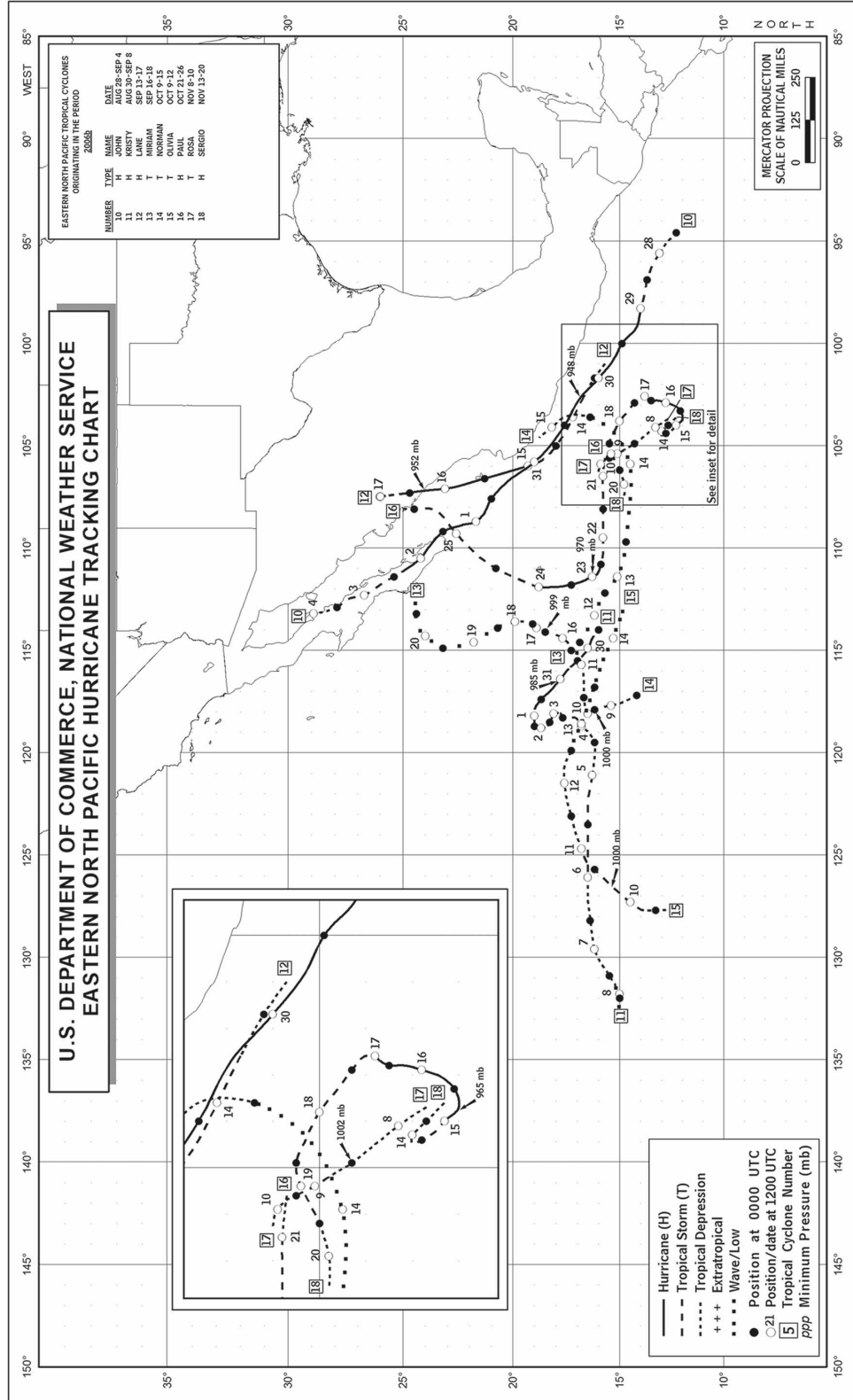
FIG. 1. (a) Track chart of the first nine eastern North Pacific tropical storms and hurricanes of 2006. (b) Track chart of the final nine eastern North Pacific tropical storms and hurricanes of 2006.
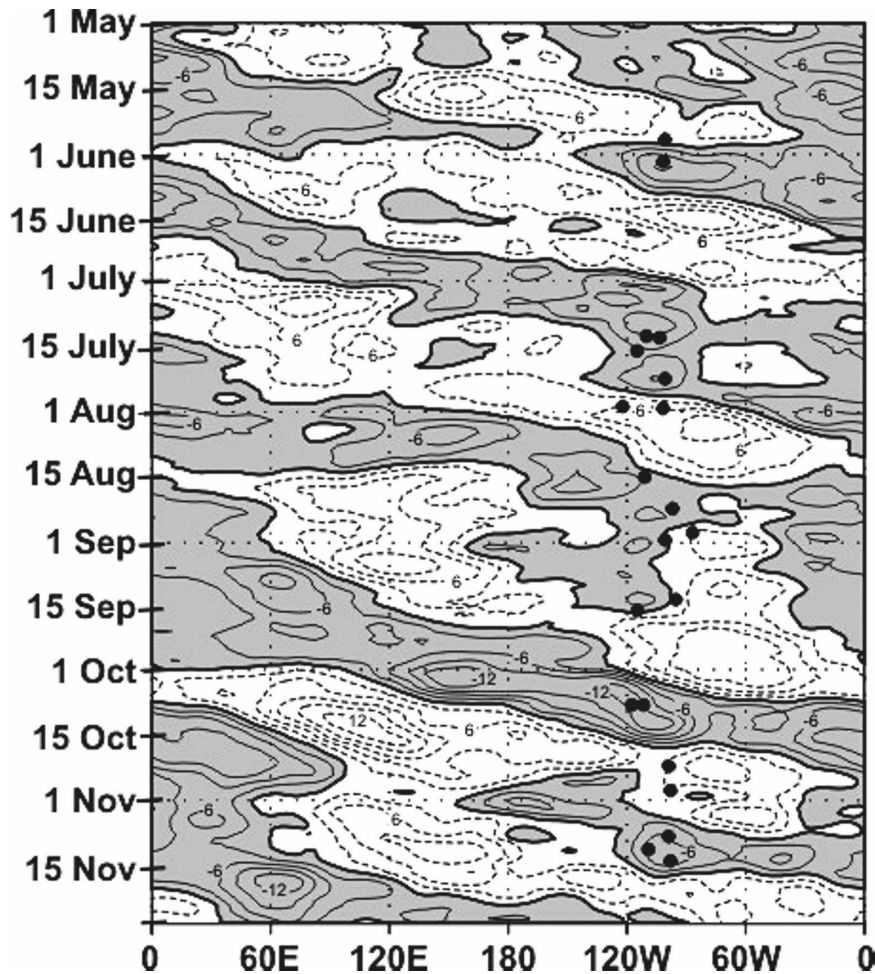
Fig. 1. (*Continued*)

FIG. 2. Five-day running mean time–longitude sections of the 200-mb velocity potential anomalies averaged from 5°N to 5°S calculated from daily anomalies during May–October 2005. Anomalies are departures from the 1971–2000 base period daily means. The contour interval is 2×10^6 m^2 s^{-1}. Negative anomalies are shaded. Superimposed dots indicate the approximate time and longitude of formation of each named storm in the eastern North Pacific during 2006. Note that most of the storms developed during upper-level divergent phases of the MJO over the eastern North Pacific, as indicated by the negative anomalies. (Graphic courtesy of the Climate Prediction Center, National Centers for Environmental Prediction.)

other three days before dissipating on 20 July about 1300 n mi east of the Hawaiian Islands.

There were no surface reports of winds of tropical storm force associated with Carlotta. Rainfall accumulations along the Pacific coast of Mexico attributable to the cyclone were less than 25 mm. There were no reports of damage or casualties due to Carlotta.

d. Hurricane Daniel, 16–26 July

Daniel, the strongest hurricane of the season, formed from a tropical wave that moved westward from the coast of Africa on 2 July. The wave crossed the Atlantic Ocean and Caribbean Sea with little deep convection

and reached the eastern North Pacific Ocean on 12 July. As the wave continued westward, convection increased beginning on 13 July, and the system showed signs of convective organization starting on 15 July. It is estimated that the wave spawned a tropical depression near 1800 UTC 16 July about 455 n mi south-southwest of Manzanillo.

The cyclone moved westward in a light vertical shear environment to the south of a large subtropical ridge. It strengthened into a tropical storm on 17 July and into a hurricane on 18 July. Daniel turned west-northwestward on 20 July and intensification was briefly halted by an eyewall replacement cycle. Strengthening resumed after the cycle, and it is estimated that Daniel
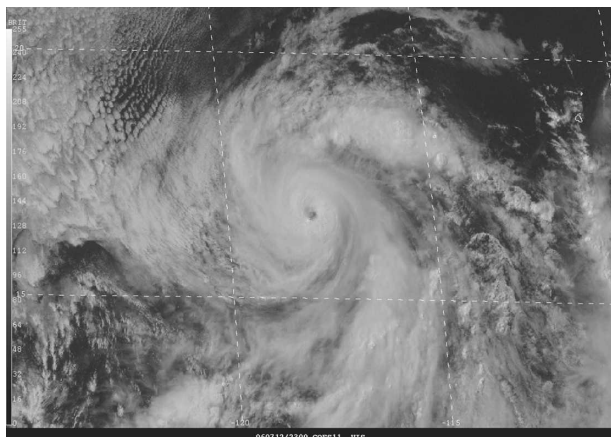
FIG. 3. *GOES-11* visible image of Hurricane Bud at 2300 UTC 12 Jul 2006, as it was nearing an intensity of 100 kt.
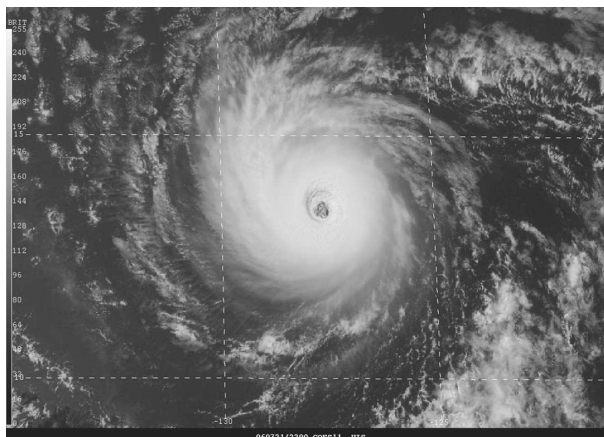

FIG. 4. *GOES-11* visible image of Hurricane Daniel at 2200 UTC 21 Jul 2006, close to its peak intensity of 130 kt.

became a category 4 hurricane later that day about 965 n mi southwest of Cabo San Lucas. Daniel turned westward on 21 July during a second eyewall replacement cycle. After this cycle, the hurricane reached an estimated peak intensity of 130 kt around 0000 UTC 22 July. Figure 4 is a visible satellite image of Daniel around the time of maximum intensity. A slow weakening trend began later that day as Daniel moved over progressively cooler sea surface temperatures.

The hurricane turned west-northwestward on 23 July, and early the next day it crossed 140°W into the central North Pacific basin, where the Central Pacific Hurricane Center assumed forecast responsibility. It turned westward and decelerated as the subtropical ridge to the north weakened. Due to a combination of cooler waters and increasing easterly shear, Daniel weakened into a tropical storm on 25 July and a tropical depression on 26 July. The cyclone degenerated to a nonconvective remnant low near 0000 UTC 27 July about 645 n mi east-southeast of Hilo, Hawaii. The low moved generally west-northwestward until it dissipated the next day about 220 n mi east-southeast of Hilo.

e. Tropical Storm Emilia, 21–28 July

A tropical wave moved across northern South America into the eastern North Pacific Ocean on 16 July, and continued steadily westward for the next several days with little change in organization. By early on 20 July, a surface low pressure system developed along the wave axis about 370 n mi south of Acapulco, and deep convection began to increase. The low pressure area turned northwestward early on 21 July and thunderstorm activity increased and became organized enough for the system to be classified as a tropical depression at 1200 UTC, about 350 n mi south-southwest of Acapulco.

After the cyclone turned northwestward, convective banding features gradually developed and became better defined, and the system strengthened into a tropical storm by 0600 UTC 22 July about 350 n mi south of Manzanillo. For the next five days, Tropical Storm Emilia alternated between a west-northwestward and north-northwestward direction around the southwestern periphery of a large subtropical ridge centered over the southwestern United States and northern Mexico. Around 0600 UTC 22 July, Emilia passed about 150 n mi southwest of Manzanillo and likely produced wind gusts to tropical storm force along the southwestern coast of mainland Mexico. Emilia reached its first peak intensity of 55 kt at 1800 UTC 23 July about 190 n mi west-southwest of Manzanillo. An increase in vertical wind shear caused the cyclone to weaken for the next 24 h. Emilia began to reintensify early on 25 July as the shear relaxed, and the cyclone reached its second peak intensity of 55 kt early on 26 July. Later that day, the center of Emilia passed about 50 n mi southwest of Cabo San Lazaro on the southwestern coast of the Baja California peninsula of Mexico. Outer rainbands affected southern portions of Baja California with locally heavy rainfall and tropical storm force winds. By early on 27 July, Emilia turned toward the west-northwest and moved over much cooler water off the west coast of Baja California, and began to rapidly weaken. Emilia became a tropical depression by 1200 UTC 27 July and degenerated into a nonconvective remnant low pressure system at 0600 UTC on 28 July about 280 n mi west of Punta Eugenia. The low moved slowly westward for the next two days before turning sharply northward early on 30 July. It dissipated at 1200 UTC 31 July about 430 n mi west-southwest of San Diego, California.

Tropical storm–force winds were reported along the

southern tip of Baja California and southwestern coast of Baja California. Between 2200–2300 UTC 25 July, Cabo San Lucas (elevation 223 m) reported a 10-min average wind of 37 kt, and a 37-kt wind with a gust to 48 kt was reported at Puerto Cortes, Mexico (elevation 42 m) at 0730 UTC 26 July.

News reports indicate rainfall totals of 3–5 in. were measured at a few locations across the southern Baja California peninsula with 5 in. reported in Cabo San Lucas. More rain likely occurred in the higher elevations of southern Baja. The reports also indicated there were a few minor floods in and around the Cabo San Lucas area. Although minor damage occurred to buildings and above-ground utility lines, no significant damage was reported in the main tourist regions of the city. Several marinas along the southern tip of Baja California, however, received minor damage from waves and were closed for about two days. There were no reports of casualties associated with Emilia.

f. Tropical Storm Fabio, 31 July–3 August

Fabio formed from a tropical wave that emerged from the coast of Africa on 15 July and then moved westward across the Atlantic Ocean and Caribbean Sea while generating only a few showers and thunderstorms. There was a temporary burst of deep convection when the wave crossed Central America on 25 July, but it weakened on 26–27 July as the system entered the eastern North Pacific. Convection redeveloped on 28 July, when a weak area of low pressure formed approximately 450 n mi southwest of Manzanillo. Showers and thunderstorms slowly became better organized over the next three days as the low moved northwestward. By 1800 UTC 31 July, the system acquired sufficient organized deep convection to be designated as a tropical depression while centered 850 n mi southwest of the southern tip of Baja California. The cyclone became a tropical storm 6 h later and reached its peak intensity of 45 kt at 1200 UTC 1 August. As Fabio moved due westward south of a midtropospheric ridge, the cyclone encountered increasing easterly vertical shear and a more stable air mass. These environmental factors ultimately resulted in Fabio weakening back to a depression at 0000 UTC 3 August about 1400 miles east of Hilo Hawaii. Fabio degenerated into a remnant low at 0000 UTC 4 August, continued westward, and became an open trough by 0000 UTC 6 August.

g. Tropical Storm Gilma, 1–3 August

Gilma developed from a tropical wave that moved off the west coast of Africa on 17 July and moved across the Atlantic Ocean and Caribbean Sea with no signs of development. The wave entered the eastern North Pacific Ocean on 25 July, and the associated disturbed weather began showing signs of organization on 29 July. Deep convection waxed and waned for a few days as the system slowly became more organized under marginally favorable upper-level winds. By 0000 UTC 1 August, the system had acquired enough deep convection and sufficient organization to be classified as a 30-kt tropical depression while centered about 360 n mi southwest of Acapulco.

Despite moderate easterly shear, convection developed close to the center, resulting in strengthening to a tropical storm at 1200 UTC 1 August. Throughout its lifetime, Gilma moved on a west-northwestward track along the southern periphery of a midlevel ridge located over northwestern Mexico and Baja California. Despite several bursts of deep convection close to the circulation center, persistent easterly shear prevented further intensification. By 0600 UTC 2 August, the low-level center became completely exposed and Gilma weakened to a tropical depression. Gilma degenerated to a remnant low at 0000 UTC 4 August about 375 n mi west-southwest of Manzanillo. The remnant low lasted for another 24 h before dissipating on 5 August about 325 n mi south-southwest of the southern tip of Baja California.

h. Hurricane Hector, 15–23 August

Hector formed from a tropical wave that exited the west coast of Africa on 31 July. The system was rather ill defined as it moved over the eastern Atlantic, but it became more convectively active and easier to track after entering the eastern Caribbean Sea. On 10 August, the wave moved across Central America and entered the eastern North Pacific. Showers and thunderstorms gradually increased as the system passed south of the Gulf of Tehuantepec, and a broad low pressure area developed about 375 n mi south of Acapulco on 13 August. Over the next couple of days, the system gradually became better organized and developed into a tropical depression around 1800 UTC 15 August about 650 n mi south-southwest of the southern tip of Baja California.

Moving west-northwestward to the south of a midlevel high pressure ridge that extended from northern Mexico westward into the northeastern Pacific Ocean, the depression quickly strengthened and became a tropical storm at 0000 UTC 16 August. Despite initially being in an environment of moderate north-northeasterly shear, Hector was able to steadily strengthen, and it reached hurricane status by 0600 UTC 17 August. While continuing west-northwestward, the hurri-

cane quickly intensified, and it is estimated that Hector reached its peak intensity of 95 kt at 0600 UTC 18 August, while centered about 900 n mi southwest of the southern tip of Baja California.

Hector remained a category 2 hurricane for about 24 h. It encountered lower sea surface temperatures and some westerly shear thereafter. Hector weakened below hurricane strength by 1200 UTC 20 August. Shortly after this time, the storm approached a weakness in the subtropical ridge near 135°W, slowed, and turned toward the northwest. On 21 August, deep convection became confined to the northeast portion of the circulation due to southwesterly shear from a small upper-tropospheric low pressure system to the northwest of Hector. The shear was not strong enough to cause dissipation, and the cyclone remained a tropical storm with 45-kt winds for about 24 h. After the remaining shower and thunderstorm activity dissipated on 22 August, the cyclone turned westward in response to low-level easterly flow. Hector weakened to a tropical depression at 0000 UTC 23 August, and to a remnant low 6 h later. The remnant circulation of Hector dissipated on 24 August about 750 n mi east of the Hawaiian Islands.

i. Hurricane Ileana, 21–27 August

The wave that spawned Ileana moved off the west coast of Africa on 8 August. Only isolated convection formed near the wave axis as it traversed the Atlantic basin for the next week or so. This system entered the eastern North Pacific Ocean on 16 August and convection increased somewhat around the wave axis. A weak low formed from the wave on 19 August. As the low moved west-northwestward south of the Gulf of Tehuantepec, thunderstorms increased on 20 August but remained disorganized. However, deep convection consolidated near the low overnight and it is estimated that a tropical depression formed about 300 n mi south-southwest of Acapulco at 1200 UTC 21 August.

Low vertical wind shear and very high sea surface temperatures contributed to a rapid intensification of the depression. It became a tropical storm 6 h after formation, reached hurricane status the next day and strengthened into a major hurricane about 48 h after genesis. Midtropospheric ridging over Mexico forced the system to move northwestward from the time of formation until near peak intensity. On 23 August, the center of Ileana passed about 50 n mi south of Socorro Island, where hurricane-force wind gusts occurred. The hurricane reached its peak intensity of 105 kt at 1200 UTC 23 August and maintained that intensity for the rest of the day. Figure 5 is a satellite image of Ileana at 1730 UTC 23 August.
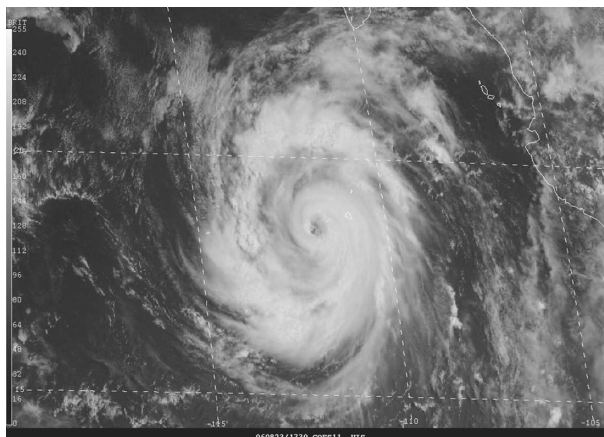

FIG. 5. *GOES-11* visible image of Hurricane Ileana at 1730 UTC 23 Aug 2006, around the time of its peak intensity of 105 kt.

Ileana commenced a slow weakening on 24 August as the tropical cyclone encountered cooler waters. Since the vertical wind shear remained light, this weakening was protracted over the next few days. As midlevel ridging to its north slowly weakened, the tropical cyclone decelerated while maintaining a west-northwestward to northwestward heading. Sea surface temperatures along the track finally decreased enough on 26 August to weaken Ileana into a tropical storm. Deep convection diminished markedly later that day as water temperatures dropped below 24°C and the tropical storm became a tropical depression early on 27 August about 550 n mi west of Cabo San Lucas. Ileana degenerated into a large remnant low at 1800 UTC 27 August, and the low moved slowly westward for a couple of days before dissipating on 29 August.

There were two observing platforms that reported tropical storm–force winds in Ileana. A Mexican Navy surface site on Socorro Island (elevation 35 m) measured 15-min sustained winds of 51 kt and gusts to 67 kt, with a pressure of 999.8 mb noted between 1500 and 1530 UTC 23 August. The vessel Cosco Panama (call sign A8HR7) reported 41-kt winds and a pressure of 1007 mb at 1800 UTC the following day about 140 n mi northeast of Ileana's center.

j. Hurricane John, 28 August–4 September

A tropical wave that departed western Africa on 17 August and entered the eastern North Pacific Ocean late on 24 August appears to be responsible for the formation of John. The cloud pattern, which was not impressive during the system's trek across the Atlantic basin, almost immediately showed signs of organization when the wave crossed into the Pacific. In fact, a Dvorak satellite classification of the system was done

around 0000 UTC 25 August, when the system was located just to the west of Costa Rica. Tropical cyclone formation is infrequent so far east in the basin, and there was little or no additional development while the system moved west-northwestward to the south of Central America over the next few days. On 27 August, curved bands of deep convection became better defined over the area to the south-southeast of the Gulf of Tehuantepec, and by 0000 UTC 28 August the system became sufficiently well organized to warrant designation as a tropical depression about 235 n mi south of Salina Cruz, Mexico. A continued increase in organization occurred, and the cyclone became a tropical storm by 1200 UTC 28 August.

A weak midlevel ridge was situated over Mexico, and the flow to the south of this ridge guided John northwestward to west-northwestward at 6–10 kt for several days. On this track, the center of the cyclone moved roughly parallel to, but not far offshore of the coast of mainland Mexico. Meanwhile, low vertical shear and a very warm ocean promoted significant intensification. John became a hurricane by 1200 UTC 29 August, and strengthened into a major hurricane just 12 h later. The storm's peak intensity of 115 kt (category 4 on the Saffir–Simpson hurricane scale) was reached around 1800 UTC 30 August. Weakening to below major hurricane status took place over the next day or so, probably due to at least one eyewall replacement. During this time, John's eye came within about 50 n mi of the coastline between Manzanillo and Lazaro Cardenas early on 31 August. On 1 September, the hurricane reintensified to category 3 status while headed in the general direction of Baja California. Late on 1 September, the tropical cyclone turned toward the north-northwest as the midlevel ridge to the north of the hurricane weakened slightly. The 10–12 n mi diameter eye of John made landfall in extreme southern Baja California at Cabo del Este, about 40 n mi northeast of Cabo San Lucas, around 0200 UTC 2 September. Although there had been some slight weakening, the hurricane's maximum winds were estimated to be near 95 kt at landfall. John moved northwestward near or just inland of the eastern coastline of the Baja peninsula, with the center of the weakening hurricane passing near La Paz shortly before 1200 UTC 2 September. John then moved up the hilly Baja California peninsula while continuing to weaken; it became a tropical storm by 1800 UTC 2 September, and eventually weakened to a tropical depression by 0000 UTC 4 September. The cyclone dissipated near the east coast of the north-central Baja California peninsula shortly after 1200 UTC 4 September.

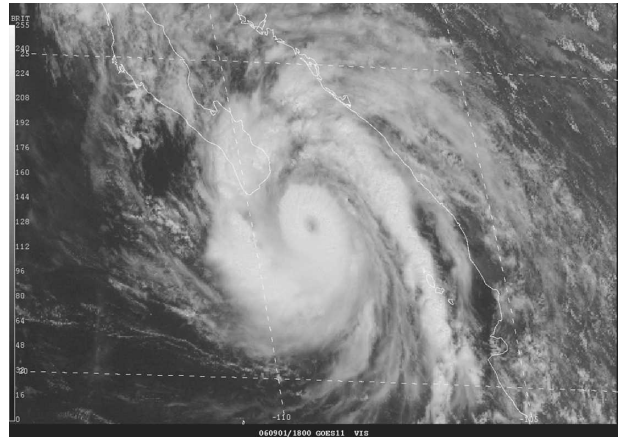The 115-kt estimated maximum intensity of this hurricane is based on a 700-mb flight-level wind of 126 kt

FIG. 6. *GOES-11* visible imagery of Hurricane John at 1800 UTC 1 Sep 2006, about 8 h before landfall in extreme southern Baja California. At this time the estimated intensity was 95 kt.

from the AFRC at 1256 UTC 30 August, a lowest 150-m average wind speed of 131 kt from a dropsonde at about the same time, and Dvorak intensity estimates of 115 kt from both the Tropical Analysis and Forecast Branch (TAFB) and Satellite Analysis Branch (SAB) at 1800 UTC 30 August. The lowest aircraft-measured central pressure was 950 mb at 1254 UTC 30 August. Since the central pressure was falling prior to the time of this observation, and the plane departed the storm shortly thereafter, it is presumed that the pressure was a little lower, 948 mb, at 1800 UTC that day—which is the estimated lowest central pressure for the life of the hurricane. No ground-based stations reported hurricane-force winds. However, the 95-kt estimate of John's strength at landfall in southern Baja California is consistent with AFRC flight-level winds of 102 kt about 8 h before landfall (Fig. 6 is a visible satellite image near that time) and images from the Los Cabos radar that showed the eyewall structure being maintained, or becoming even a little better defined, up until the time that the center crossed the coast (Fig. 7).

Selected observations from land stations appear in Table 2. The strongest winds observed over land were from the La Paz Observatory, where maximum sustained winds of 45 kt with a gust to 57 kt were reported. A rainfall total of 317.5 mm was measured at Los Planes, with nearly 280 mm of this total falling in a 24-h period.

According to press reports, John caused five deaths, all in Baja California. Two-hundred homes were reported to have been destroyed in the vicinity of La Paz. Over 250 homes were damaged or destroyed in the city of Mulege, located on the eastern coast of south-central Baja California. Heavy rains resulted in the overflow of the Iguagil dam in Comundu, which isolated 15 towns
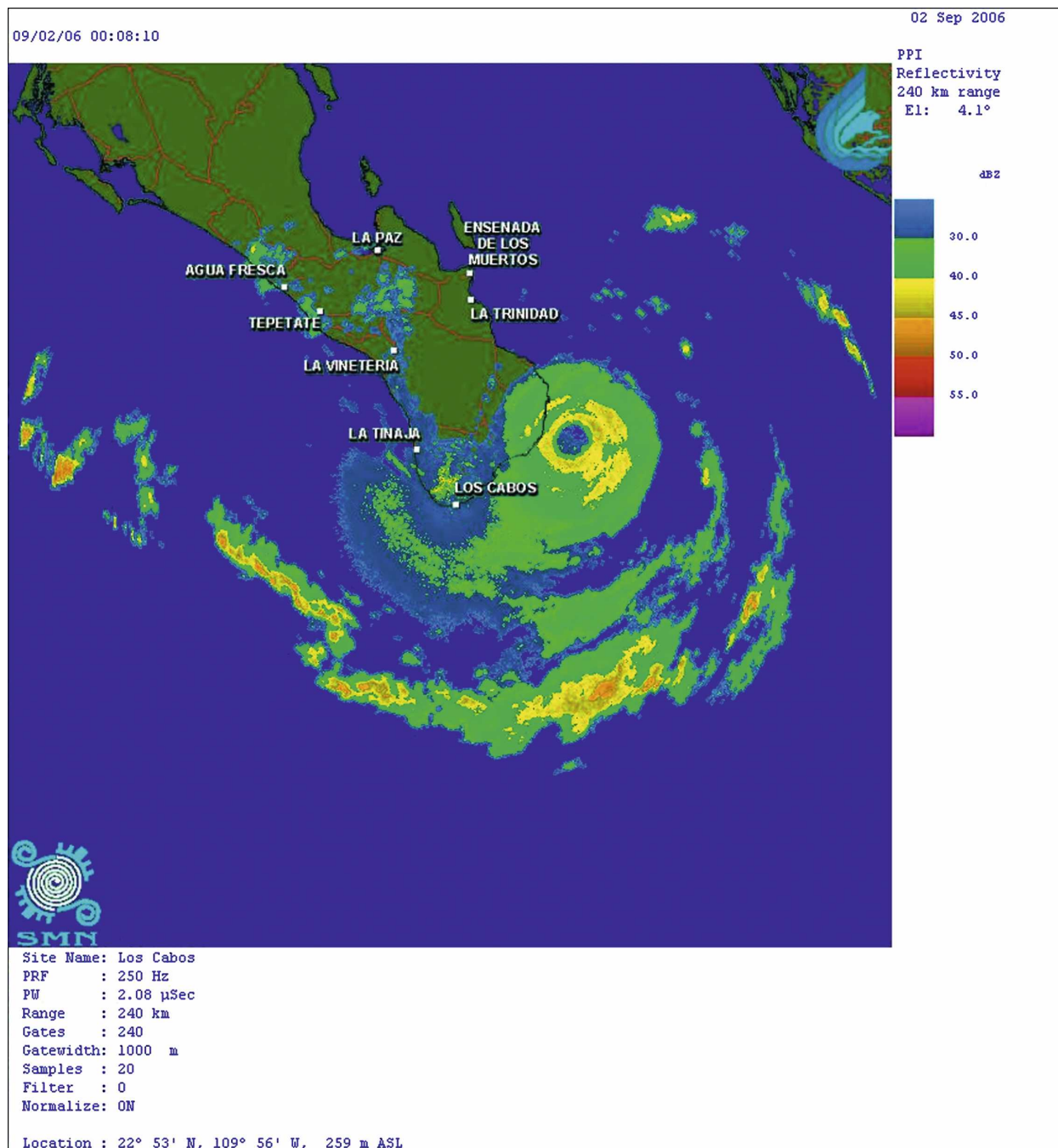
FIG. 7. Image from the Meteorological Service of Mexico's Los Cabos radar at 0008 UTC 2 Sep 2006, showing the well-defined eyewall of Hurricane John shortly before landfall in southern Baja California.

due to 1.2-m floodwaters. Winds and rains destroyed crops in large areas and killed many livestock in southern Baja California. Although the eye of the hurricane remained offshore of mainland Mexico, John affected the coast with very heavy rains and strong winds. A 3-m storm surge was reported in Acapulco, causing flooding of coastal roads in that area; however, the reported surge may have actually been due to the combined effects of waves and tides. Heavy rains produced mud slides in the Costa Chica region of Guerrero, which left around 70 communities isolated. Moisture and locally heavy rains also spread over portions of northwestern Mexico and the southwestern United States. Twenty neighborhoods were flooded by rainfall from the rem-

TABLE 2. Selected surface observations for Hurricane John, 28 Aug–4 Sep 2006.

Location (Mexico)	Min SLP		Max surface wind speed			Tot rain (mm)
	Time/date	Pressure (mb)	Time/date*	Sustained (kt)	Gust (kt)	
Ciudad Constitución	2200 UTC 2 Sep	990.4	1550 UTC 2 Sep	23	34	
Ciudad Constitución (EMA)		997.8		12	34	
La Paz	0930 UTC 2 Sep	986.8	1000 UTC 2 Sep	45	57	
Loreto						94.7
Puerto Cortés	2100 UTC 2 Sep	999.7	1530 UTC 2 Sep	31	42	
San Jose del Cabo						143**
San Jose De Los Planes						317.5
Santa Rosalía	1200 UTC 3 Sep	995.3	1200 UTC 3 Sep	34	45	146.6
Santiago						160.5
Topolobampo			1130 UTC 2 Sep		36	

 * Time/date is for sustained wind when both sustained and gust are listed.
** The 24-h total.

nants of John in Ciudad Juarez, located across the border from El Paso, Texas. Around 76 mm of rain fell in El Paso, causing some flooding and closure of roads in that area.

k. Hurricane Kristy, 30 August–8 September

Kristy developed from a tropical wave that crossed the west coast of Africa on 13 August and was identified by a large swirl of low clouds and little convection. The wave moved westward for two weeks across the Atlantic Ocean, the Caribbean Sea, and a good portion of the eastern North Pacific. There was very little deep convection associated with the wave until it reached Central America on 22 August. The wave continued westward and it was not until 29 August that the showers became persistent and began to show signs of organization. Based on Dvorak classifications, it is estimated that a tropical depression formed at 0000 UTC 30 August about 520 n mi southwest of the southern tip of Baja California. Six hours later, it became a tropical storm.

Kristy strengthened further as it moved slowly toward the northwest and became a hurricane at 0600 UTC 31 August. It reached its estimated peak intensity of 70 kt and a minimum pressure of 985 mb at 1200 UTC on the same day, when an eyelike feature was observed on microwave imagery. Steering currents then collapsed and Kristy began to meander. It then weakened because of northeasterly wind shear caused by outflow associated with Hurricane John, which was approaching Baja California. A ridge built to the north of the cyclone and Kristy began to move slowly westward, fluctuating in intensity between storm and depression status until 0600 UTC 8 August when it became a remnant low. The low continued to move slowly westward and degenerated into a wave on 9 September.

l. Hurricane Lane, 13–17 September

Lane developed from a tropical wave that departed the west coast of Africa on 31 August and entered the eastern North Pacific basin on 10 September. The system gradually became better organized during the next three days, leading to the formation of a tropical depression by 1800 UTC 13 September, centered about 100 n mi southwest of Acapulco. Weak wind shear and warm waters aided the cyclone in reaching tropical storm intensity early on 14 September. Steered west-northwestward and roughly parallel to the Pacific coast of Mexico by a midlevel ridge centered to its north, Lane continued to gradually strengthen that day. Intensification was more rapid on 15 September, and Lane became a hurricane by 1200 UTC that day while centered about 80 n mi west of Manzanillo. Turning toward the north-northwest around the southwestern periphery of the ridge, the center of Lane passed about 30 n mi west of Cabo Corrientes, Mexico, later that day. The hurricane continued to strengthen and its eastern eyewall impacted the Islas Marias very early on 16 September while Lane was at category 2 intensity; the center of Lane passed just west of the Islas Marias.

As a large midlatitude trough deepened over the western United States, Lane was drawn northward near the mouth of the Gulf of California. A distinct eye appeared on satellite and radar imagery (from Guasave, Mexico) as Lane strengthened some more, and the hurricane reached its peak intensity of 110 kt by 1200 UTC 16 September. This intensity is based on a blend of subjective Dvorak estimates at 1200 UTC ranging from 102 to 115 kt. Little change in the intensity of Lane occurred before it made landfall, as a category 3 hurricane with winds of 110 kt, at 1915 UTC that day on the Pacific coast of mainland Mexico, in the state of Sinaloa along the Peninsula de Guevedo about 15 n mi
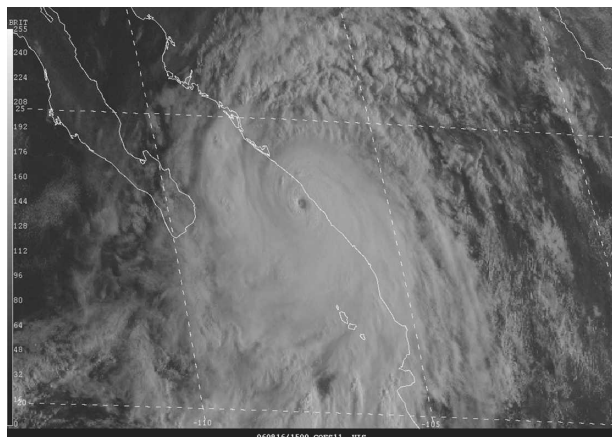
FIG. 8. *GOES-11* visible imagery of Hurricane Lane at 1500 UTC 16 Sep 2006, about 4 h before landfall. The estimated intensity is 110 kt.

southeast of El Dorado. The relatively small cyclone weakened quickly after moving inland over the rugged terrain of western Mexico. Lane weakened to a tropical storm early on 17 September, and the circulation dissipated later that day. Some of the remaining moisture contributed to enhanced rainfall over portions of northern Mexico and southern Texas.

Just prior to landfall at 1915 UTC, a reconnaissance aircraft made one penetration of the center at about 1800 UTC and measured a central pressure of 955 mb via dropsonde. The actual central pressure at that time, however, was probably slightly lower (estimated to be 954 mb) since the center dropsonde also measured a surface wind of 23 kt. Wind data from only one pass through the center are inconclusive about the intensity of Lane at landfall. The aircraft measured a maximum flight-level wind of 110 kt at 700 mb, corresponding to about 100 kt at the surface. A dropsonde in the eyewall measured a surface wind of 108 kt, but surface estimates based on low-layer profile averages were not available. Even though these limited data do not confirm that Lane had maximum sustained surface winds of 110 kt at landfall, the landfall intensity is kept at 110 kt based on the satellite estimates and the low central pressure reported by the aircraft. Figure 8 is a visible satellite image of Lane shortly before landfall.

Damage reports indicate that Lane produced strong winds and flooding over many areas along and near the Pacific coast of Mexico, including locations well removed from the landfall location, even as far southeast as Acapulco. Very few surface observations, however, are available. A 24-h total of 260 mm of rain was reported at San Lorenzo in the state of Sinaloa. A temporary tower, operated by the NOAA Earth System Research Laboratory (ESRL), was placed at Estacion

Obisbo about 10 n mi inland from the landfall point of the center, where the elevation is 27 m. Prior to being blown down in the eyewall, the tower measured a 1-min sustained surface wind of 81 kt with a gust to 105 kt at 1930 UTC 16 September; a sea level pressure of 966 mb was measured at the same location at 1945 UTC. Storm surge observations are not available.

Media reports indicate that Lane was directly responsible for four fatalities due to floods and mud slides and that damage was heaviest in the landfall area in the Mexican state of Sinaloa. Many streets and homes were flooded in El Dorado and Culiacan, to the north of where the center made landfall, and in Mazatlan, southeast of where the center came ashore. Large rural areas were also flooded, severely impacting the agricultural industry. Numerous roads were washed out, isolating several communities, and a bridge between Culiacan and Mazatlan was destroyed. Impacts were also significant much farther south and east along the coast of Mexico, even though the center of Lane remained just offshore there. Hundreds of homes were evacuated, many crops were destroyed, and some roads were damaged due to floods and mud slides in the coastal states of Michoacan, Colima, and Jalisco. The combination of high waves and heavy rains left more than a foot of water in some streets of Acapulco (even farther southeast in the state of Guerrero), where about 200 homes were flooded and a mud slide caused one of the fatalities. Just offshore from Acapulco a boat capsized, leaving one person reportedly missing.

m. Tropical Storm Miriam, 16–18 September

Miriam developed within a broad area of disturbed weather that represented a northward extension of the intertropical convergence zone to the west of Hurricane Lane. One disturbance within this trough, associated with the tropical wave in front of Lane, briefly became organized on 14 September, but soon weakened. A second disturbance formed a little to the northeast of the first on 15 September and developed a distinct closed circulation late in the day. By 0000 UTC 16 September, this system had enough convective organization to be classified as a tropical depression, about 440 n mi southwest of Cabo San Lucas, Mexico, and about 500 n mi west-southwest of Lane.

Initially, the depression moved slowly northeastward, embedded in southwesterly low- to midlevel flow feeding into Hurricane Lane. The depression strengthened and became a tropical storm near 1200 UTC 16 September, about 400 n mi southwest of Cabo San Lucas, and 12 h later it reached its peak intensity of 40 kt. Persistent northeasterly wind shear, as well as low-level

inflow from a cool and stable environment to the north, limited further development. By midday on 17 September the low-level circulation became decoupled from the deep convection, the latter racing off to the west of the former. The circulation then began to slowly spin down, with winds falling below storm strength by 0600 UTC the following day. Shortly thereafter, Miriam degenerated to a remnant low, which moved generally northward toward the Baja California peninsula before dissipating on 21 September a short distance offshore.

The center of Miriam passed about 30 n mi to the east of the automated station at Clarion Island late on 16 September. This station (elevation 60 m) reported a maximum 15-min mean wind of 31 kt, with a gust to 43 kt at 0830 UTC 17 September, and a minimum pressure of 1003.2 mb at 0030 UTC 17 September.

n. Tropical Storm Norman, 9–15 October

Norman formed from a tropical wave that moved westward from the coast of Africa on 21 September. The wave crossed the tropical Atlantic Ocean and Caribbean Sea with little convection, reaching the eastern North Pacific on 1 October. It moved slowly westward and showed increasing convection beginning on 5 October. By 8 October, the wave was in the eastern portion of a large and complex area of disturbed weather, which included a system to the west that became Tropical Storm Olivia. The eastern system showed signs of convective organization that day, and additional organization resulted in the formation of a tropical depression near 0000 UTC 9 October about 665 n mi southwest of Cabo San Lucas.

The depression moved slowly north-northwestward and became a tropical storm 12 h after genesis. Norman reached a peak intensity of 45 kt early on 10 October. Southwesterly vertical wind shear then displaced the convection to the northeast of the center, and Norman weakened to a depression later that day as it turned east-northeastward. Continued shear caused the cyclone to degenerate to a low pressure area on 11 October about 460 n mi southwest of Cabo San Lucas.

The low pressure area moved east-southeastward on 12–13 October, followed by an eastward motion on 14 October. This motion was due to the low interacting with a broad area of disturbed weather near the coast of southwestern Mexico. During the interaction, convection became reorganized near the center of the low, and it is estimated that Norman regenerated into a tropical depression around 0000 UTC 15 October while centered about 175 n mi south-southeast of Manzanillo. The cyclone moved northward and then northwestward inside the cyclonic envelope of the larger disturbance

until it abruptly dissipated late on 15 October about 20 n mi south of Manzanillo.

It should be noted that the exact fate of the center of Norman on 15 October is uncertain. Conventional satellite imagery suggests the center may have moved inland east of Manzanillo. However, surface observations do not support a landfall, and the center was too disorganized to be easily tracked in microwave satellite imagery. Therefore, the best estimate is that the center dissipated over water as it approached Manzanillo. While Norman produced some locally heavy rains over portions of southwestern Mexico, there were no reports of damage or casualties.

o. Tropical Storm Olivia, 9–12 October

Olivia originated from a tropical wave that moved off the west coast of Africa on 18 September. Minor flareups of convection occurred on 19 and 20 September when the wave was located south and southwest, respectively, of the Cape Verde Islands. Otherwise, the wave marched uneventfully westward across the tropical Atlantic Ocean and northern South America remaining devoid of any significant deep convection. Upon reaching the eastern North Pacific waters on 29 September, deep convection began to slowly increase and by early on 5 October a broad surface low pressure system developed along the wave axis. Over the next few days, westerly vertical wind shear inhibited significant development of the system. As the low pressure system continued to move slowly westward the shear relaxed somewhat, and deep convection gradually became organized into a long curved band over the northern semicircle. It is estimated that a tropical depression formed by 1800 UTC 9 October 2006, about 1180 n mi west-southwest of the southern tip of Baja California, Mexico.

The tropical depression turned slowly northward and moved into a region of weaker vertical wind shear, strengthening into a tropical storm at 0600 UTC 10 October. Shortly after obtaining tropical storm status, Olivia began to gradually accelerate toward the northeast and reached its estimated peak intensity of 40 kt just 6 h later. However, almost as quickly as Olivia strengthened, it weakened as it moved into a region of stronger upper-level southerly winds and drier air, which caused deep convection to decrease and become displaced away from the low-level circulation center. The cyclone became a tropical depression by 1200 UTC 11 October about 900 n mi west-southwest of southern Baja California. The depression turned eastward and strong vertical shear caused the cyclone to degenerate into a nonconvective remnant low pressure system

early on 13 October. The low moved east-southeastward, and by 0000 UTC 15 October, it was absorbed into the southern portion of the larger remnant circulation of former Tropical Storm Norman when the latter system was centered about 130 n mi south-southwest of Manzanillo. It is possible that the remnants of Olivia played a role in the redevelopment of Norman back into a tropical cyclone just 6 h later.

p. Hurricane Paul, 21–26 October

Paul formed from a tropical wave that emerged from the west coast of Africa on 4 October. The system moved westward across the Atlantic Ocean and Caribbean Sea during the next two weeks and produced little deep convection. The wave crossed Central America on 18 October and merged with a preexisting area of disturbed weather over the eastern North Pacific on 19 October. This event resulted in the formation of a larger area of convection that extended northward to the southern coast of Mexico. An area of low pressure developed in this region on 20 October, and a tropical depression is estimated to have formed around 0600 UTC 21 October about 230 n mi south-southwest of Manzanillo.

The depression quickly became more organized and strengthened to a tropical storm only 6 h after genesis. Under the influence of increasing easterly shear associated with a mid- to upper-tropospheric ridge over Mexico, however, only modest additional development occurred during the next 24 h. As Paul reached the western periphery of the ridge late on 22 October, vertical shear decreased, and the cyclone rapidly intensified between 1800 UTC 22 October and 1200 UTC 23 October. During this 18-h period, maximum sustained winds increased from 45 to 90 kt. In addition, Paul's forward speed decreased as it began to turn toward the north. The hurricane then began to interact with a large mid- to upper-level trough off the west coast of the United States that increased westerly shear, and subsequent weakening starting late on 23 October.

After its center passed just west of Socorro Island early on 24 October, Paul became embedded within an area of deep southwesterly flow ahead of the upper-level trough and accelerated northeastward. Weakening was temporarily arrested early on 25 October due to a burst of deep convection as the cyclone approached the southern tip of Baja California.

Strong vertical shear began to displace the convection to the northeast while the center was passing about 40 n mi south of Cabo San Lucas early on 25 October. The low-level circulation became completely exposed a few hours later, and Paul weakened to a depression by

0000 UTC 26 October as it approached the coast of mainland Mexico. The increasingly shallow cyclone turned toward the north with a decrease in forward speed, and made landfall along the coast of mainland Mexico near the southern end of Isla Altamura around 0400 UTC 26 October. Paul dissipated a few hours later while centered approximately 50 n mi northwest of Culiacán near La Bahia de Santa Maria, Mexico.

Observations from aircraft include flight-level and dropwindsonde data from two missions flown by the 53rd Weather Reconnaissance Squadron of the AFRC. The estimated peak intensity of 90 kt at 1200 UTC 23 October is based on unanimous subjective Dvorak intensity estimates from TAFB, SAB, and AFWA. While subsequent subjective satellite intensity estimates indicated that Paul maintained this intensity for another 12–18 h, the best-track intensity during this period is set beneath those estimates based on the aircraft data.

Paul produced large waves and high surf over southern portions of Baja California that resulted in two deaths there. One death involved an American tourist who was swept out to sea, while the second death occurred when a fisherman was swept off rocks in high surf. Paul also produced very heavy rainfall resulting in floods in the state of Sinaloa. According to media reports, 5000 homes were damaged causing 20 000 people to be displaced. The worst flooding occurred in Villa Juarez where a canal overflowed and flooded streets with approximately 1 m of water. Two deaths occurred in the municipality of Navolato, where a truck was swept away by a swollen river, bringing the total death toll directly attributable to Paul to four.

q. Tropical Storm Rosa, 8–10 November

The development of Rosa appears to have been associated with a tropical wave that left the west coast of Africa on 22 October. While traversing the Atlantic Ocean and the Caribbean Sea, the wave remained relatively weak and somewhat difficult to track. On 3 November, the wave crossed Central America and entered the eastern North Pacific Ocean. Shower and thunderstorm activity then began to increase, and a broad low pressure area developed several hundred miles south of the Gulf of Tehuantepec on 5 November. The convection remained disorganized the next day, but gradually increased in organization on 7 November. Early the next day, convection increased significantly near the center of the low, which led to the formation of a tropical depression at 0600 UTC 8 November about 385 n mi south of Manzanillo.

The tropical cyclone moved slowly northwestward throughout its existence. Six hours after formation, sat-
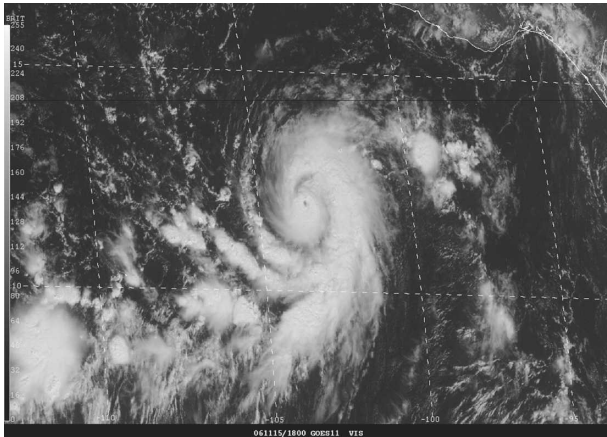
FIG. 9. *GOES-11* visible image of Hurricane Sergio at 1800 UTC 15 Nov 2006, when it had an estimated intensity of 95 kt.

est-lived November tropical cyclone on record for that basin. Sergio appears to have been spawned by a tropical wave that crossed southern Central America and entered the eastern North Pacific on 7 November. An area of cloudiness and showers associated with the wave moved slowly westward to the south of Central America and eastern Mexico over the next several days. Showers and thunderstorms became more concentrated by 12 November over an area centered roughly 350 n mi to the south of Acapulco. By 1800 UTC 13 November, when the system was a little over 400 n mi to the south of Manzanillo, it had acquired enough surface circulation and organized deep convection to be designated as a tropical depression.

Initially the cyclone was moving northwestward, but it soon stalled while strengthening into a tropical storm on 14 November. Sergio then turned toward the southeast, apparently because of the flow associated with a mid- to upper-level trough to its northeast, and continued to intensify. While situated in an environment of light vertical shear, with anticyclonic flow aloft and a generally moist troposphere, the storm became a hurricane on 15 November, and it quickly strengthened to a peak intensity of 95 kt around 1800 UTC that day. Sergio exhibited a distinct and very small eye around that time (Fig. 9). The hurricane then turned toward the northeast and north-northeast and weakened as westerly shear, associated with an upper-level trough to the northwest, increased over the tropical cyclone. By early on 17 November, the low-cloud circulation became partially exposed on the west side of the deep convection, and it is estimated that Sergio weakened to a tropical storm by 0600 UTC that day. During the next few days, an area of high pressure built to the northeast and north of the tropical cyclone, which forced the sys-

ellite intensity estimates suggest that the depression was near tropical storm strength. The appearance of the tropical cyclone on satellite imagery then degenerated somewhat due to southwesterly wind shear. Despite the shear, convection reformed near the center early on 9 November and based on QuikSCAT data the depression strengthened to a minimal tropical storm by 0600 UTC while centered about 260 n mi south-southwest of Manzanillo. The strong shear halted further intensification and Rosa remained a tropical storm for only 18 h. Rosa weakened to a tropical depression at 0000 UTC 10 November and the circulation gradually dissipated, becoming an open trough later that day while located about 215 n mi southwest of Manzanillo.

r. Hurricane Sergio, 13–20 November

Sergio was the strongest eastern North Pacific hurricane for so late in the season, and it was also the long-

TABLE 3. Homogenous comparison of official (OFCL) and CLIPER5 track forecast errors in the eastern North Pacific basin for the 2006 season for all tropical cyclones. Averages for the previous 5-yr period are shown for comparison.

	Forecast period (h)						
	12	24	36	48	72	96	120
2006 mean OFCL error (n mi)	30.2	54.5	77.4	99.7	142.3	186.1	227.5
2006 mean CLIPER5 error (n mi)	36.2	72.7	112.1	152.3	220.5	260.1	300.8
2006 mean OFCL error relative to CLIPER5 (%)	−17	−25	−31	−35	−36	−29	−24
2006 mean OFCL bias vector [°/n mi]	326/5	339/8	348/10	336/11	334/01	105/10	041/11
2006 No. of cases	341	302	264	228	159	107	71
2001–05 mean OFCL error (n mi)	35.1	60.1	82.5	102.6	144.6	191.8	231.1
2001–05 mean CLIPER5 error (n mi)	42.2	81.2	122.5	159.0	224.4	281.8	341.0
2001–05 mean OFCL error relative to CLIPER5 (%)	−17	−26	−33	−36	−36	−32	−32
2001–05 mean OFCL bias vector (°/n mi)	323/1	290/1	267/3	287/7	233/5	183/13	211/25
2001–05 No. of cases	1300	1152	1009	877	652	465	313
2006 OFCL error relative to 2001–05 mean (%)	−14	−9	−6	−3	−2	−3	−2
2006 CLIPER5 error relative to 2001–05 mean (%)	−14	−10	−8	−4	−2	−8	−12

TABLE 4. Homogenous comparison of official (OFCL) and Decay-SHIFOR5 intensity forecast errors in the eastern North Pacific basin for the 2006 season for all tropical cyclones. Averages for the previous 5-yr period are shown for comparison.

	Forecast period (h)						
	12	24	36	48	72	96	120
2006 mean OFCL error (kt)	6.8	11.2	14.6	16.1	17.8	19.3	18.3
2006 mean Decay-SHIFOR5 error (kt)	7.9	12.7	15.9	18.3	19.8	23.4	23.6
2006 mean OFCL error relative to Decay-SHIFOR5 (%)	−14	−12	−8	−12	−10	−18	−23
2006 OFCL bias (kt)	1.0	1.5	1.5	1.4	4.4	3.0	−0.4
2006 No. of cases	341	302	264	228	159	107	71
2001–05 mean OFCL error (kt)	6.2	10.8	14.3	16.5	18.7	18.3	19.3
2001–05 mean Decay-SHIFOR5 error (kt)	7.0	11.6	15.2	17.7	21.3	20.4	19.1
2001–05 mean OFCL error relative to Decay-SHIFOR5 (%)	−11	−7	−6	−7	−12	−10	+1
2001–05 OFCL bias (kt)	0.9	2.2	3.2	3.1	4.4	5.5	4.9
2001–05 No. of cases	1300	1151	1009	876	652	465	313
2006 OFCL error relative to 2001–05 mean (%)	+10	+4	+2	−2	−5	+5	−5
2006 Decay-SHIFOR5 error relative to 2001–05 mean (%)	+13	+10	+5	+3	−7	−15	+24

tem to turn toward the northwest, west, and eventually west-southwest. Although there was some slight re-strengthening on 18 November when deep convection reformed near the center, Sergio was mainly on a weak-ening trend as persistently strong shear took its toll. The cyclone weakened to a tropical depression by about 0000 UTC 20 November, and it dissipated later that day about 315 n mi southwest of Manzanillo, as the low-level circulation became stretched along a cyclonic shear axis.

3. Forecast verification

For all operationally designated tropical cyclones in its area of responsibility, the NHC issues an "official" tropical cyclone track (latitude and longitude of the circulation center) and intensity (maximum 1-min wind speed at 10 m above the surface) forecast every 6 h. These forecasts are made for the 12-, 24-, 36-, 48-, 72-, 96-, and 120-h periods from the initial synoptic time of the forecast (0000, 0600, 1200, or 1800 UTC). The forecasts are evaluated using the postseason 6-hourly best-track database for all tropical cyclones (includ-ing tropical depressions). The track error is defined as the great-circle distance between forecast and best-track positions of the tropical cyclone center, and the intensity error is the absolute value of the difference between the forecast and best-track intensi-ties.

A comparison of the average track errors for 2006 and the previous 5-yr period for the official forecasts and the CLIPER5[1] (Neumann 1972; Aberson 1998)

model forecasts is shown in Table 3, taken from Frank-lin (2007). CLIPER5 serves as a benchmark of track forecast skill. The 2006 track errors were lower than the 5-yr means at all forecast lead times, but only by 2%–6% beyond 24 h. There was a northward component in the bias of the mean track forecasts at all lead times except 96 h. The 2006 CLIPER5 track errors were lower than the 5-yr mean CLIPER5 errors at the vari-ous forecast lead times by 2%–14%. This suggests that the 2006 eastern North Pacific tropical cyclones were easier to forecast, on average. At all forecast lead times, the mean official track errors were substantially lower than the mean CLIPER5 errors indicating that the of-ficial forecasts were quite skillful.

Table 4, also from Franklin (2007) is similar to Table 3, but for intensity forecasts and it compares official forecasts to the Decay-SHIFOR5[2] (Jarvinen and Neu-mann 1979) model that serves as a benchmark of inten-sity forecast skill. Average official intensity forecasts had some skill during 2006 since the mean forecast er-rors for the year ranged from 8% to 23% lower than the corresponding SHIFOR5 errors at the various forecast times. The mean official intensity errors for 2006 were higher than the long-term (2001–05) means for 12–36 h, but were lower than the long-term means for 38–120 h. The official forecasts had a high bias at all forecast times except for 120 h. This is not greatly dissimilar to the long-term mean biases, except for the latter forecast time. Finally, it should be noted that official intensity forecast errors and forecast skill for the eastern North Pacific have not changed appreciably during the past decade (Franklin 2007).

---

[1] CLIPER5 is a 5-day version of the original Climatology and Persistence (CLIPER) model.

[2] SHIFOR5 is a 5-day version of and the original Statistical Hurricane Intensity Forecast (SHIFOR) model.

REFERENCES

Aberson, S. D., 1998: Five-day tropical cyclone track forecasts in the North Atlantic basin. *Wea. Forecasting,* **13,** 1005–1015.

Avila, L. A., R. J. Pasch, J. L. Beven, J. L. Franklin, M. B. Lawrence, S. R. Stewart, and J. Jiing, 2003: Eastern North Pacific hurricane season of 2001. *Mon. Wea. Rev.,* **131,** 249–262.

Dvorak, V. F., 1984: Tropical cyclone intensity analysis using satellite data. NOAA Tech. Rep. NESDIS 11, 47 pp.

Franklin, J. L., 2007: 2006 National Hurricane Center Forecast Verification Report. NOAA, 57 pp. [Available online at http://www.nhc.noaa.gov/verification/pdfs/Verification_2006.pdf.]

Jarvinen, B. R., and C. J. Neumann, 1979: Statistical forecasts of tropical cyclone intensity for the North Atlantic basin. NOAA Tech. Memo. NWS NHC-10, 22 pp.

Knabb, R. D., L. A. Avila, J. L. Beven, J. L. Franklin, R. J. Pasch, and S. R. Stewart, 2008: Eastern North Pacific hurricane season of 2005. *Mon. Wea. Rev.,* **136,** 1201–1216.

Levinson, D. H., 2007: East Pacific basin, overview of the 2006 season (in "State of the Climate in 2006"). *Bull. Amer. Meteor. Soc.,* **88,** S51–S54.

Madden, R. A., and P. R. Julian, 1972: Description of global-scale circulation cells in the tropics with 40-50 day period. *J. Atmos. Sci.,* **29,** 1109–1123.

Neumann, C. B., 1972: An alternate to the HURRAN (hurricane analog) tropical cyclone forecast system. NOAA Tech. Memo. NWS SR-62, 24 pp.

Saffir, H. S., 1973: Hurricane wind and storm surge. *Mil. Eng.,* **423,** 4–5.

Simpson, R. H., 1974: The hurricane disaster potential scale. *Weatherwise,* **27,** 169, 186.